J. Ocean Univ. China (Oceanic and Coastal Sea Research)
DOI 10.1007/s11802-014-2251-z
ISSN 1672-5182, 2014 13 (5): 733-741
http://www.ouc.edu.cn/xbywb/
E-mail:xbywb@ouc.edu.cn

A Numerical Study of Tidal Asymmetry: Preferable Asymmetry of Nonlinear Mechanisms in Xiangshan Bay, East China Sea

XU Peng[1)], MAO Xinyan[2), *], JIANG Wensheng[1)], and ZHOU Liangming[2)]

1) *Physical Oceanography Laboratory*, *Ocean University of China*, *Qingdao* 266100, *P. R. China*
2) *College of Physical and Environmental Oceanography*, *Ocean University of China*, *Qingdao* 266100, *P. R. China*

(Received December 17, 2012; revised February 2, 2013; accepted June 4, 2014)

Abstract *In-situ* measurements in Xiangshan Bay, the East China Sea, show that the duration of the rising tide is shorter than that of the falling tide around the bay mouth, while it becomes much longer in the inner bay. A finite volume coastal ocean model (FVCOM) with an unstructured mesh was applied to simulate the asymmetric tidal field of Xiangshan Bay. The model reproduced the observed tidal elevations and currents successfully. Several numerical experiments were conducted to clarify the roles of primary mechanisms underlying the asymmetric tidal field. According to the model results, the time-varying channel depth and nonlinear advection prefer shorter duration of the rising tide in Xiangshan Bay, while the time-varying bay width favors longer duration of the rising tide. The overtides generated by these two opposite types of nonlinear mechanisms are out of phase, resulting in smaller M_4 amplitude than the sumfold of each individual contribution. Although the bottom friction as a nonlinear mechanism contributes little to the generation of overtide M_4, it is regarded as a mechanism that could cause a shorter duration of the rising tide, for it can slow down the M_2 phase speed much more than it slows down the M_4 phase speed. The time-varying depth, nonlinear advection and bottom friction are dominating factors around the bay mouth, while the time-varying width dominates in the inner bay, causing the tidal elevation asymmetry to be inverted along the bay.

Key words FVCOM; tidal asymmetry; Xiangshan Bay; nonlinear mechanisms

1 Introduction

Astronomical tidal waves can be distorted when they propagate into coastal shelves, bays and estuaries, due to the generation of the overtides and compound tides by nonlinear mechanisms (Speer and Aubrey, 1985; Friedrichs and Madsen, 1992; Nidzieko, 2010; Song *et al.*, 2011). This distortion is characterized by tidal elevation and current asymmetry, which refers to a difference between durations of rising and falling tides, as well as a difference in durations and magnitudes of flooding and ebbing currents (Boon and Byrne, 1981; Friedrichs and Aubrey, 1988; de Swart and Zimmerman, 2009). The asymmetry of tides plays an important role in the transport and accumulation of suspended matters and sediments in tidal inlets and basins (Lanzoni and Seminara, 1998; Wang *et al.*, 2002; Nidzieko, 2012; van Maren and Gerritsen, 2012).

Xiangshan Bay, the biggest aquaculture base in Zhejiang province, is located on the east coast of China, with an average water depth of 10 m and a total area of about 560 km^2. The bay is narrow and semi-enclosed, and has a horizontal scale of 70 by 10 km (Fig.1). Topography in the bay is characterized by two shallower ends and a deeper middle portion, with some deep spots scattered along the bay. About 1/3 of the total bay area is mudflats, most of which are distributed around the head, with only a few distributed along the edge of the channel (Dong and Su, 1999a). Wind and waves are weak in the bay (Cao *et al.*, 1995), while tides are very energetic and highly asymmetric (Zhu and Cao, 2010), and dominate the distribution pattern of suspended matters and sediments (Gao *et al.*, 1990). In a semi-diurnal system such as Xiangshan Bay (Dong and Su, 1999a, b), the tidal asymmetry is mainly caused by the interaction between the principal semidiurnal tide M_2 and its first overtide M_4 generated by the nonlinear tidal process (Speer and Aubrey, 1985).

The tidal asymmetry has been studied by various researchers. Parker (1991) proposed that four primary physical mechanisms are responsible for the generation of shallow water tides, which are the time-varying channel depth and the time-varying embayment width in the continuity equation, and the nonlinear advection and bottom friction terms in the momentum equations. In shallow water systems where bottom friction is conspicuous, the trough of tidal waves propagates slower than the crest due to the stronger bottom friction during low tide, which results in a shorter duration of the rising tide (LeBlond,

* Corresponding author. Tel: 0086-532-66782269
E-mail: maoxinyan@ouc.edu.cn

1978; Friedrichs and Aubrey, 1994; Lanzoni and Seminara, 2008; Wang *et al.*, 2002). However, the existence of large intertidal flats may significantly change the asymmetric tides, and makes the duration of the rising tide longer than that of the falling tide (Shetye and Gouviea, 1992). Friedrichs and Madsen (1992) proposed that the relative importance of the time-varying channel depth and the time-varying embayment width determines the asymmetry of tidal elevation. The duration of the rising tide is shorter when the time-varying depth dominates over the time-varying width; otherwise, it is longer.

Until now, the studies on asymmetric tide in Xiangshan Bay have been rare. Dong and Su (1999a, b) published the only paper regarding the generation mechanism of overtide M_4 in the Bay. They reported that the overtide M_4 grows from 0.02 m at the mouth to 0.36 m at the head based on the observations, and they analyzed the different effect of nonlinear mechanisms using a depth-averaged numerical model.

In Dong and Su's study (1999a, b), only the effect of nonlinear mechanisms on the amplitude of overtide M_4 was discussed. Thus, it is necessary to understand how each nonlinear mechanism affects the tidal elevation asymmetry through examining both amplitudes and phases of semidiurnal tide M_2 and overtide M_4. In this study a finite-volume coastal ocean model (FVCOM) was employed to simulate the highly asymmetric tides and to investigate how each of the primary nonlinear mechanisms affects the tidal asymmetry in Xiangshan Bay. The paper is organized as follows: Section 2 introduces the main characteristics of the asymmetric tides in Xiangshan Bay based on the observations. The model configuration and validation are presented in Section 3. Section 4 is the result analysis by comparing the benchmark and various sensitivity experiments. The conclusions are drawn in Section 5.

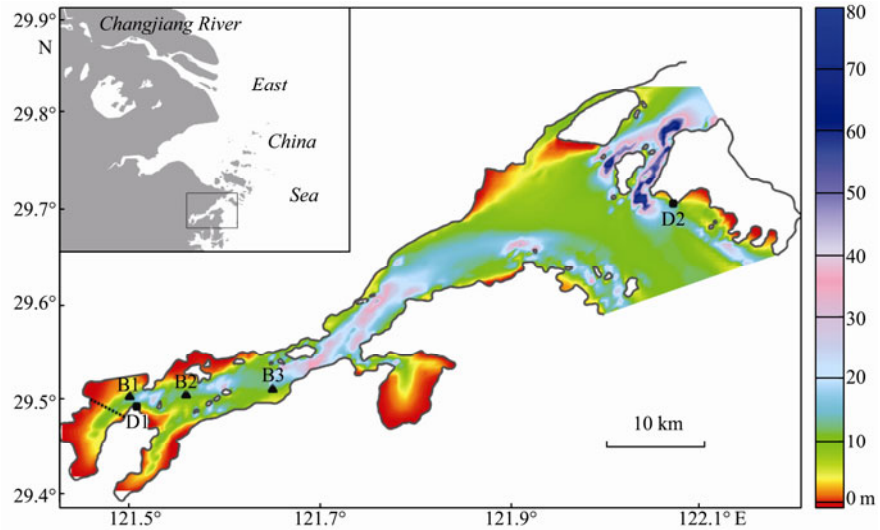

Fig.1 The bathymetry of Xiangshan bay. The areas covered by red and yellow colors are the mudflats. B1-B3 are the locations of the tidal level and current mooring sites while only tidal levels are measured at D1 and D2. The dashed line at the head represents the cross-section in Fig.8 and the small panel shows the location of the bay in the East China Sea.

2 Field Observations in Xiangshan Bay

Several cruises have been carried out to collect tidal level and current data in Xiangshan Bay since 2008 (Table 1). All the high-frequency sampling data were averaged over a 10-minute interval, and also vertically averaged on current profiles.

Table 1 Stations and instrumentation

Station	Depth (m)	Duration (mm.dd.yy)	Instrument	Sampling interval
D1	8.7	01.23.08 – 02.01.08	RBR TGR2050 TD	10 min
B1/B2/B3	11.4/11.5/12.5	12.21.10 – 12.23.10 09.14.11 – 09.15.11	RDI WH 600 kHz ADCP / RBR XR420 CTD	2 s/1 s
D2	3.0	04.10.12 – 04.11.12	RBR TGR2050 TD	1 min

Considering the phase difference between tidal elevation and current, it can be seen that Xiangshan Bay belongs to a standing wave system and the tidal current in the inner bay is rectilinear due to the shoreline limitation. There are two other apparent and important characteristics of the tide in Xiangshan Bay. One is that the tidal elevation changes from a shorter duration of the rising tide at the mouth to a longer duration at the head. By taking stations D2 and B2 to represent the mouth and head of the Bay (Fig.1), respectively, it can be seen that the tidal range increases from the mouth (about 4.0 m) to the head (about 6.5 m) with an increasing degree of tidal asymmetry (Figs.2a, 2b). The tidal elevation at station D2 shows weak asymmetry, with the duration of the falling tide ex-

ceeding that of the rising tide by about 1 hour. However, the asymmetry of tidal elevation is inverted at station B2, with a duration of the rising tide 2-hour longer than that of the falling tide. The other characteristic is that the peak magnitudes of flooding and ebbing currents are almost identical though the durations of them are quite different. Additionally, a big and a tiny peak exist for the flooding current, while only one peak occurs for the ebb current (Fig.2c).

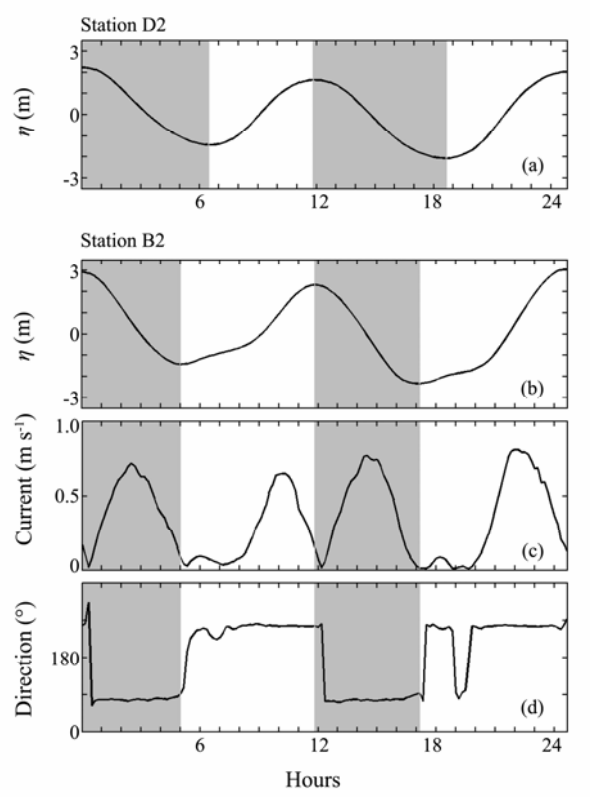

Fig.2 Observed tidal elevations at station D2(a), station B2(b), and the magnitude (c) and the direction (d) of vertically-mean tidal currents at station B2. The gray color represents the duration of the falling tide.

3 Model Configuration and Validation

3.1 Model Configuration

FVCOM is a free surface primitive equation model, developed by the UMASSD-WHOI development team, and has the capability to simulate asymmetrical tidal fields in small inlets (Chen *et al.*, 2003; Chen *et al.*, 2006a, b; Chen *et al.*, 2007; Chen *et al.*, 2009; Huang *et al.*, 2008). The model equations are solved on an unstructured boundary-fitted triangular mesh in horizontal and on a generalized terrain-following sigma coordinate system in vertical (Pietrzak *et al.*, 2002; Chen *et al.*, 2003).

The computational domain of this study is bounded by the coastline on the west, and the open boundary on the shelf of the East China Sea (Fig.3). The horizontal resolution at the open boundary is 10 km and gradually increases to 200 m in Xiangshan Bay. The model bathymetry inside the bay was digitized from nautical charts (China Maritime Safety Administration, 2008), while bathymetry outside Xiangshan Bay was extracted from the SKKU bathymetry data (Choi *et al.*, 2002). Eight primary tidal constituents (M_2 S_2 N_2 K_2 K_1 O_1 P_1 Q_1) from OTPS (Oregon State University Tidal Prediction Software) were specified at the open boundary. The water density field was set to be constant and the wind forcing was neglected in numerical experiments. These assumptions were taken considering the shallowness of, the small runoff into and the calm winds over the bay all year round (Dong and Su, 2000; Zhang *et al.*, 2008).

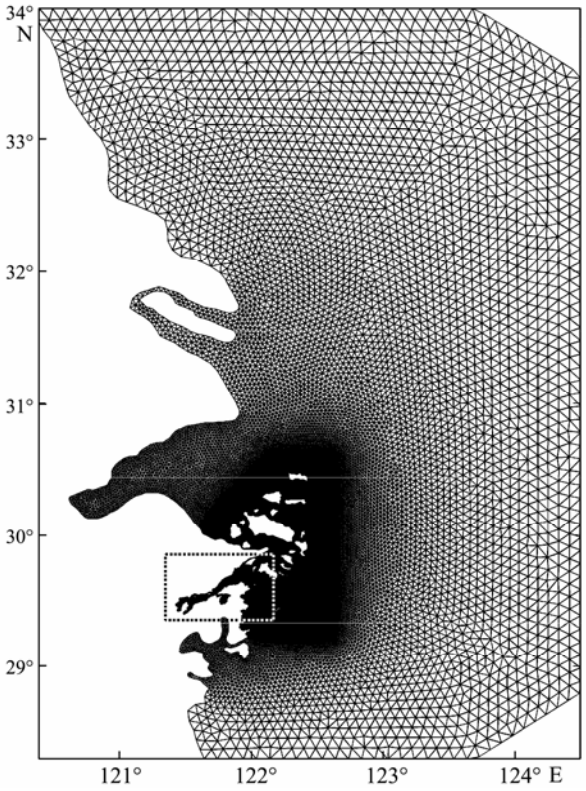

Fig.3 The unstructured grid of FVCOM. The dashed line in the figure delineates the location of Xiangshan Bay.

FVCOM includes a wetting/drying scheme to simulate the flooding and ebbing processes over the intertidal flat, which has been applied to verify the role of intertidal flats in channel dynamics (Zheng *et al.*, 2003; Huang *et al.*, 2008). In this study, a depth of 5 cm was chosen as a critical value to determine if a cell is wet or dry.

A two-zone parameterization of the bottom drag coefficient was introduced into this model (Sheng and Wang, 2004; Nicolle and Karpytchev, 2007). Outside the bay, the conventional value of $\sim 2.5\times10^{-3}$ was used, while inside the bay, $\sim 0.3\times10^{-3}$ was set based on the ADCP data (Xu *et al.*, 2012).

3.2 Model Validation

Fig.4 shows the simulated co-tidal charts of M_2 and M_4 tides in Xiangshan Bay. The amplitude of M_2 increases from 1.5 m at the mouth to 2.2 m at the head, in accor-

dance with that reported by Dong and Su (1999a, b). The amplitude of M_4 grows in a pattern similar to that of M_2 along the bay, starting with 0.02 m at the mouth and increasing to 0.33 m at the head, which is also consistent with Dong and Su's (1999a, b) observations except for a 3 cm difference at the head. Thus the model performs well for the simulation of overtide M_4 in Xiangshan Bay.

Time series of calculated and observed tidal elevation and current in Xiangshan Bay are compared (Fig.5). To quantify the difference between the model results and observations, the relative error (E) and the correlation coefficient (r) are computed as follows (Spitz and Klinck, 1998):

$$E = 100\% \frac{\sum_{i=1}^{n}(M-O)^2}{\sum_{i=1}^{n}(|M-\overline{O}|^2+(O-\overline{O})^2)}, \quad (1)$$

$$r = \frac{\sum_{i=1}^{n}(M-\overline{M})(O-\overline{O})}{[\sum_{i=1}^{n}(M-\overline{M})^2\sum_{i=1}^{n}(O-\overline{O})^2]^{1/2}}, \quad (2)$$

where M and O are the calculated results and the observed data and the overbar represents the temporal average. The relative error (E) gives a measure of the relative difference in amplitudes while the correlation coefficient (r) measures the phase difference between the simulated results and the observed data.

For the tidal elevation comparison, the relative errors range from 2.5% to 4.4%, and the correlation coefficients are very close to 1.0. However, the relative errors range from 10.8% (Figs.5e) to 36.6% (Fig.5b), and the correlation coefficients vary from 0.8 to 0.9 for the tidal current comparison. It is clear that the model does well in reproducing the asymmetric tide in Xiangshan Bay (Figs.5a and 5g). How nonlinear mechanisms affect the asymmetric tidal field in Xiangshan Bay is investigated using the model results in the following section.

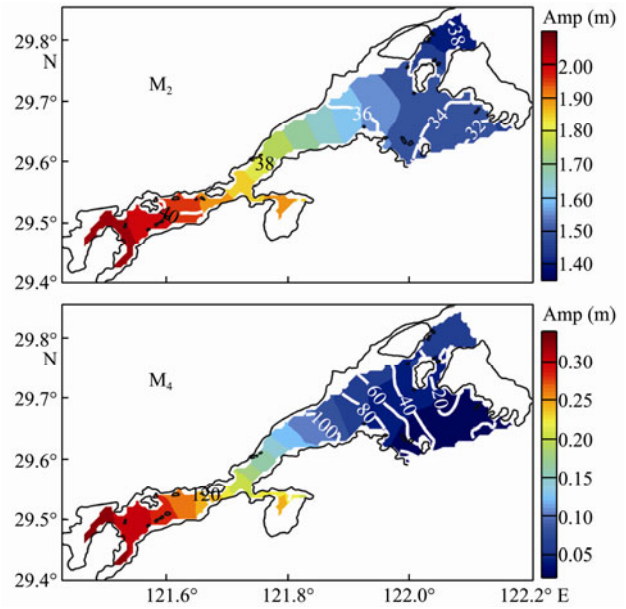

Fig.4 Co-tidal charts of M_2 (upper panel) and M_4 (lower panel). The colors show the amplitudes (in meters), and the white lines are the co-tidal phase lines (in degrees). The white areas between coastlines and the colored area are the intertidal zone.

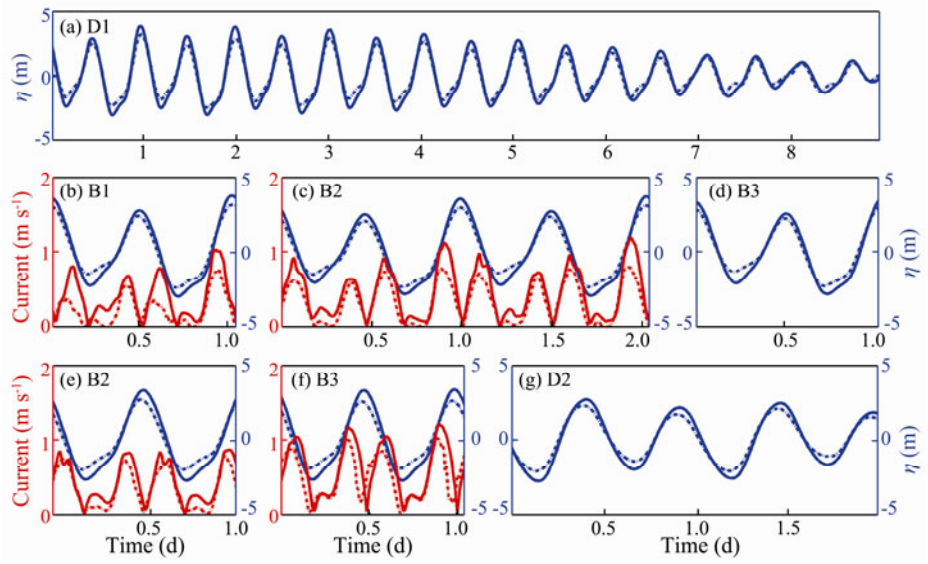

Fig.5 Time series of the observed (dashed line) and calculated results (solid line). The blue color represents tidal elevation, while the red represents tidal current. Panels (a)–(g) show the results of the 2008 cruise at station D1, the 2010 cruise at stations B1, B2, B3, the 2011 cruise at stations B2, B3, and the 2012 cruise at station D2, respectively.

4 Discussion of Nonlinear Mechanisms

The benchmark and four sensitivity experiments were conducted to examine the contributions of nonlinear mechanisms to the tidal elevation asymmetry in Xiangshan Bay (Table 2). The considered mechanisms include those associated with bottom friction, morphology, bathymetry,

and nonlinear advection. Two parameters are used in the discussion, one is the relative phase between M_2 and M_4, $2g_{M2}-g_{M4}$; the other one is H_{M4}/H_{M2}, *i.e.*, the amplitude ratio of M_4 to M_2 tides. The sign of the former indicates the asymmetry direction, while the latter represents the degree of tidal asymmetry. If the relative phase is positive, the duration of the rising tide is shorter than that of the falling tide, and vice versa (Speer and Aubrey, 1985).

Table 2 The description of the sensitivity experiments

Experiment	Description
Benchmark experiment	The model configuration in Section 3
EXP 1	Increase C_d in Xiangshan Bay from 0.3×10^{-3} to 2.5×10^{-3}
EXP 2	No intertidal flat in Xiangshan Bay
EXP 3	Decrease the main channel depth by 3 m
EXP 4	No nonlinear advection in Xiangshan Bay

Fig.6 shows the variations of harmonic constants of M_2 and M_4 constituents and the two parameters from mouth to head in the benchmark experiment. Besides the increasing trend as mentioned in Section 3.2, it can be found that the relative phase decreases from 67° around the mouth to −37° in the inner bay, indicating the inversion of tidal asymmetry along the bay (Fig.6a). The reversal point is at the location 19 km from the bay mouth, which divides the bay into two opposite systems. In the outer bay, the tidal elevation asymmetry is weak due to the small amplitude

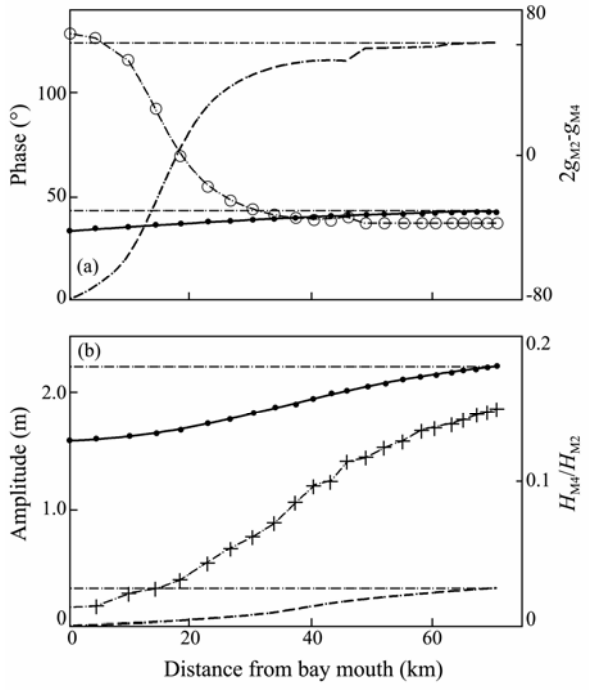

Fig.6 The calculated M_2 and M_4 harmonic constants along the bay in the benchmark experiment. Panel (a) presents the M_2 phase (solid line), the M_4 phase (dashed line), and the relative phase (line with circles), while panel (b) shows the M_2 amplitude (solid line), the M_4 amplitude (dashed line), and the amplitude ratio of M_4 to M_2 (line with crosses). The horizontal dashed lines mark the M_2 and M_4 phases and amplitudes at the bay head.

of M_4 tide (Fig.6b), while the asymmetry becomes stronger in the inner bay because the amplitude ratio increases by approximately 15 times along the bay.

4.1 Role of Bottom Friction

The bottom friction plays two opposite roles in the tidal asymmetry, the dissipation and the generation of high-frequency tides. In EXP 1, the bottom drag coefficient in Xiangshan Bay increases from 0.3×10^{-3} of the benchmark value to 2.5×10^{-3}. The enhanced bottom damping effect reduces phase speeds of both M_2 and M_4 tides (Fig.7a). The M_2 phase difference between the mouth and the head is about 11° larger compared to that in the benchmark case. However, there is little phase discrepancy of M_4 tide between these two experiments. Since the bottom friction slows down the propagation of M_2 tide much more than it does for M_4 tide, the relative phase in the bay increases significantly, implying a reverse trend of the tidal elevation asymmetry at the head. The inverse point in EXP 1 moves 20 km further toward the head due to the increase of the relative phase in the inner bay. Therefore the bottom friction plays an important role in generating a shorter rising tide in Xiangshan Bay.

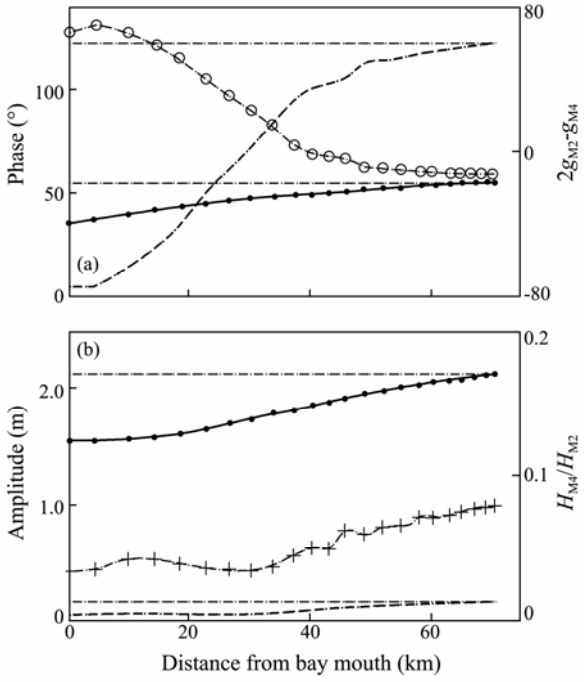

Fig.7 to the same as in Fig.6, but for EXP 1.

The bottom damping effect can not only slow down the phase speeds of M_2 and M_4 tides but also reduce their amplitudes (Parker, 1991). In EXP 1, the M_2 amplitude at the head decreases by only 5%, while the M_4 amplitude drops by 48%, and hence the amplitude ratio decreases by one half from 0.15 to 0.08 (Fig.7b). This suggests that the bottom friction damps the M_4 amplitude more than it damps the M_2 amplitude and results in a smaller amplitude ratio. Therefore, the strong bottom friction can decrease the degree of the tidal elevation asymmetry, and

vice versa. It should be noted that the reduction of the tidal amplitude in EXP 1 has little influence on the width of intertidal flat (decreasing by only 4%). The average lower low tides of the benchmark case and EXP 1 are almost the same, both of which occur on the slope of the channel rather than on the side of the flat where a small water-level variation would correspond to a great change in flooded area (Fig.8).

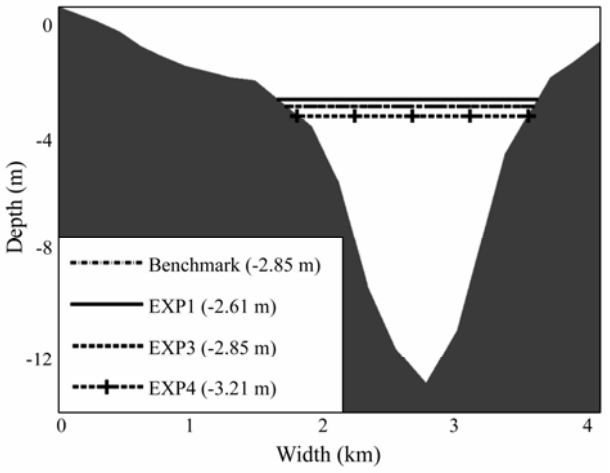

Fig.8 The average lower low spring tides of the experiments (numbers in parenthesis) in the cross-section marked by the dashed line in Fig.1.

In addition to its damping effect, the nonlinear mechanism of bottom friction also causes the interaction between tides due to the quadratic form of bottom friction ($\tau_b=C_d|U|U$). However, as Parker (1991) pointed out, the quadratic bottom friction cannot generate overtide in a semidiurnal-tide dominating system if there is no mean flux. For this reason, the nonlinear effect of bottom friction has no contribution to the asymmetric tide.

4.2 Effect of the Intertidal Storage Volume

According to previous studies (Speer and Aubrey, 1985; Friedrichs and Madsen, 1992), the intertidal storage volume plays a crucial role in the systems where the duration of the rising tide is shorter. In EXP 2, the intertidal flat (Fig.1) was removed from the computational domain in order to examine its contribution to the asymmetric tide in Xiangshan Bay.

The removal of this intertidal flat enhances the convergence of the bay, leads to a faster M_2 phase speed (Lanzoni and Seminara, 1998), and decreases the M_2 phase difference by 3˚ (Fig.9a). However, due to the absence of the intertidal flat, the M_4 phase sharply increases from 1˚ at the mouth to over 120˚ around the head in the benchmark experiment, but remains about 35˚ along the bay in EXP 2. Owing to the large M_4 phase variation, the relative phase in the bay becomes negative. The results of EXP 2 indicate that the time-varying width, dominant in the inner bay, prefers a longer duration of rising tide.

Tidal amplitudes are quite different between EXP 2 and the benchmark experiment. More energy is transferred from M_2 to M_4 tides in EXP 2 than in the benchmark experiment (Fig.9b). A further comparison shows that the absence of the intertidal flat not only inverts the tidal elevation asymmetry in the inner bay, but also promotes the energy shift from M_2 to M_4. It is indicated that M_4 overtide generated by time-varying width and other nonlinear mechanisms may be out of phase.

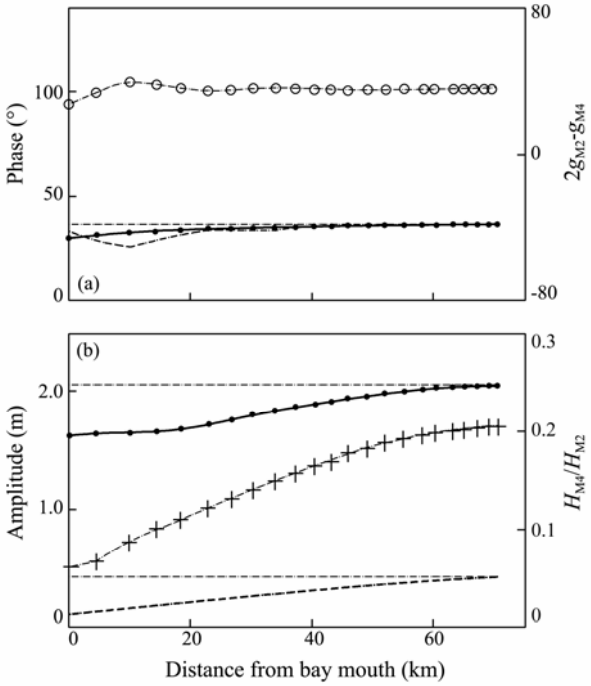

Fig.9 The same as in Fig.6, but for EXP 2.

4.3 Nonlinear Effect of Time-Varying Depth

Time-varying depth is mainly caused by sea surface oscillation. EXP 3 was set up to investigate the contribution of the time-varying depth to the tidal elevation asymmetry in Xiangshan Bay, in which the channel depth was reduced by 3 m and the bathymetry of the intertidal flat remained the same as in the benchmark experiment. The reduction of the channel depth can increase the convergence of the bay, and can also enhance the dissipation by bottom friction. Owing to these two opposite effects, the average lower low tide in EXP 3 remained the same as that in the benchmark experiment (Fig.8), which guarantees that the effects of the time-varying width between the two experiments are almost the same. Compared with the benchmark experiment, the M_2 phase speed in EXP 3 slowed down and the phase difference increased by 10˚ due to the shoaling in the bay (Fig.10a). The M_4 phase remained almost the same at the mouth and head, while the spatial gradient from the outer to the inner bay became moderate, and the inversion point was pushed 11 km toward the head. This distribution pattern of the tides and the relative phases were very similar to that in EXP 1, suggesting that the time-varying depth plays a similar role as bottom friction in affecting tidal asymmetry.

Nevertheless, the contribution of the bottom friction to the tidal elevation asymmetry in Xiangshan Bay is due to

its linear damping effect, while the time-varying depth is a nonlinear mechanism responsible for the energy transfer from M_2 to M_4 tides. Compared to the benchmark experiment, the EXP 3 results show that the M_2 amplitude increases at both the mouth and the head, but the M_4 amplitude increases at the mouth and decreases at the head. Thus the relative phase of EXP 3 presents a similar pattern to that of the benchmark experiment (Fig.10b).

The variations of the amplitude ratio along the bay confirm that the time-varying depth is a nonlinear mechanism which prefers longer duration of rising tide. Therefore, the time-varying depth would promote the generation of overtide M_4 at the mouth but suppress it in the inner bay.

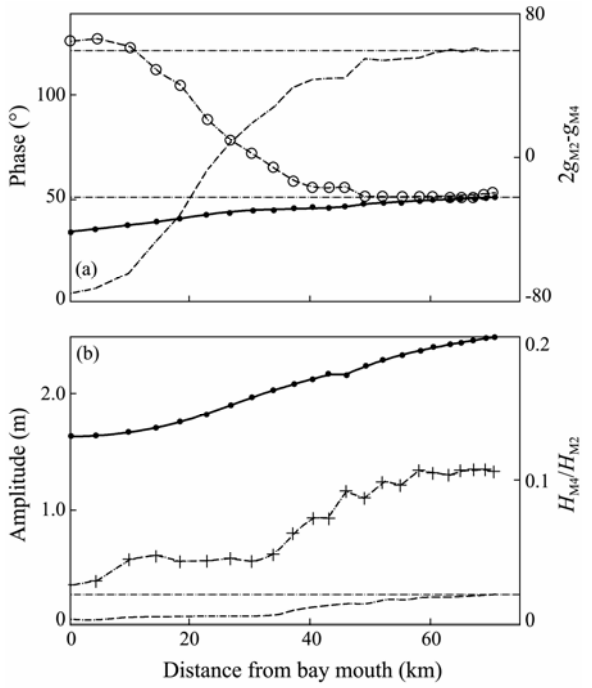

Fig.10 To the same as in Fig.6, but for EXP 3.

4.4 Effect of Nonlinear Advection

In EXP 4, the horizontal advection terms in the momentum equations were neglected, and the results were compared with the benchmark experiment to assess the contribution of nonlinear advection to the tidal elevation asymmetry in Xiangshan Bay.

Fig.11a shows that the absence of nonlinear advection corresponds to a 3° smaller phase difference of M_2 tide and a much greater phase difference of M_4 tide between EXP 4 and the benchmark experiments, and causes the negative relative phase all over the bay. The tidal elevation at the mouth changes from that of a shorter rising tide in the benchmark experiment to a longer rising tide in EXP 4. It indicates that the nonlinear advection prefers shorter rising tide and can counteract the effect of the intertidal volume storage like the time-varying depth. However, the nonlinear advection regulates the relative phase by different means from the time-varying depth. The former exerts a greater influence on the M_4 tide phase while the latter affects the M_2 tide phase more.

Little influence of nonlinear advection has been found on the M_2 amplitude by comparisons. However, the M_4 amplitude in EXP 4 increases significantly at the head, which enhances the degree of the tidal elevation asymmetry (Fig.11b). Owing to the enhanced intensity of the longer-rising-tide system in the inner bay, the influence of the intertidal flat transforms the system around the mouth from a shorter to longer rising tide. The tidal range becomes larger in EXP 4, but the width of the intertidal flat increases by only 6% (Fig.8). The contribution of the intertidal volume storage in EXP 4 is similar to that in the benchmark experiment.

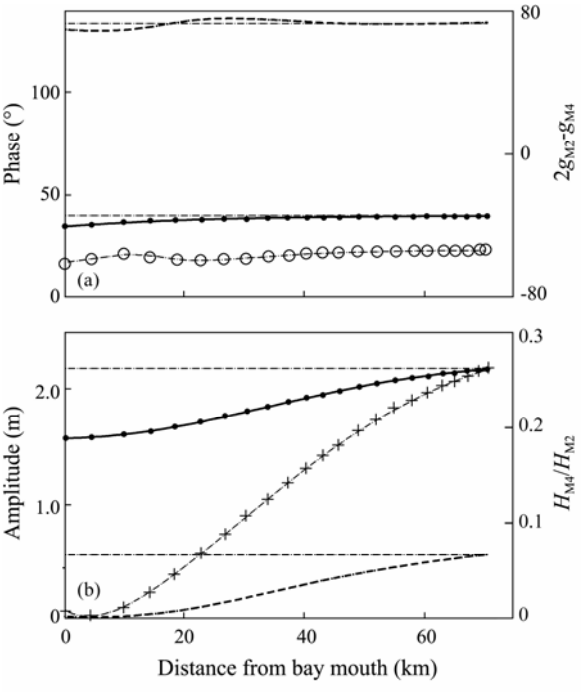

Fig.11 To the same as in Fig.6, but for EXP 4.

5 Conclusions

Observations show that the tide in Xiangshan Bay is highly asymmetric, and the tidal elevation asymmetry reverses along the bay. In this paper, a finite-volume coastal ocean model was employed to study the physical mechanisms behind this asymmetry. The contribution of each primary nonlinear mechanism to the asymmetry in tidal field is discussed by conducting the sensitivity experiments.

According to the different effects on the relative phase between M_2 and M_4 tides, the nonlinear mechanisms responsible for the tidal elevation asymmetry in Xiangshan Bay are sorted into two categories. The time-varying width prefers a longer duration of rising tide, while the time-varying depth and nonlinear advection prefers a shorter duration. Although the nonlinear effect of bottom friction is not associated with the generation of overtide M_4, its damping effect causes a shorter duration of rising tide.

The inversion of the tidal elevation asymmetry is caused by the changes in dominant nonlinear mechanisms

along the bay. The time-varying depth and nonlinear advection dominate in the outer bay and result in a shorter duration of rising tide there. However, the asymmetry of the tidal elevation reverses along the bay because of the large intertidal volume storage at the head. The M_4 phase adjusts itself rapidly along the bay. Because the overtides generated by the nonlinear mechanisms of the two categories are out of phase, the amplitude of M_4 generated by all the nonlinear mechanisms is smaller than the sum of that generated by each individual.

Acknowledgements

This study is sponsored by the National Natural Science Foundation of China (41106006) and the National Key Technology R&D Program of China (2011BAC03 B02). We also thank Dr. Changsheng Chen for providing the FVCOM code.

References

Boon, J. D., and Byrne, R. J., 1981. On basin hypsometry and the morphodynamic response of coastal inlet systems. *Marine Geology*, **40**: 27-48, DOI: 10.1016/0025-3227(81)90041-4.

Cao, X. Z., Tang, L. M., and Zhang, Y. X., 1995. Analyses of the hydrography features and the ability for containing contaminator for port Xiangshan. *Donghai Marine Science*, **13** (1): 10-19 (in Chinese with English abstract).

Chen, C. S., Beardsley R. C., and Cowles, G., 2006b. An unstructured grid, finite-volume coastal ocean model (FVCOM) system. *Oceanography*, **19** (1): 78-89, DOI: 10.5670/oceanog.2006.92.

Chen, C. S., Beardsley, R. C., and Cowles, G., 2006a. An unstructured grid, finite-volume coastal ocean model: FVCOM user manual. SMAST/UMASSD, New Bedford, Mass, 318pp.

Chen, C. S., Huang, H. S., Beardsley, R. C., Liu, H. D., Xu, Q. C., and Cowles, G., 2007. A finite volume numerical approach for coastal circulation studies: Comparisons with finite difference models. *Journal of Geophysical Research*, **112**, C03018, DOI: 10.1029/2006JC003485.

Chen, C. S., Liu, H. D., and Beardsley, R. C., 2003. An unstructured grid, finite-volume, three-dimensional, primitive equations ocean model: Application to coastal ocean and estuaries. *Journal of Atmospheric and Oceanic Technology*, **20**: 159-186.

Chen, C. S., Malanotte-Rizzoli, P., Wei, J., Beardsley, R. C., Lai Z., Xue, P. F., Lyu, S. J., Xu, Q. C., Qi, J., and Cowles, G. W., 2009. Application and comparison of Kalman filters for coastal ocean problems: An experiment with FVCOM. *Journal of Geophysical Research*, **114**, C05011, DOI: 10.1029/2007JC004548.

China Maritime Safety Administration, 2008. *Xiangshan Gang and Approaches*. China Navigation Publications Press, Tianjin.

Choi, B., Kim, K., and Eum, H. M., 2002. Digital bathymetric and topographic data for neighboring seas of Korea. *Journal of Korean Society of Coastal Ocean Engineers*, **14**: 41-50 (in Korean with English abstract).

de Swart, H. E., and Zimmerman, T. J. F., 2009. Morphodynamics of tidal inlet systems. *Annual Review of Fluid Mechanics*, **41**: 203-229, DOI: 10.1146/annurev.fluid.010908.165159.

Dong, L. X., and Su, J. L., 1999a. Tide response and wave distortion in Xiangshan Bay I: Observation and analysis. *Acta Oceanogica Sinica*, **21**: 1 (in Chinese with English abstract).

Dong, L. X., and Su, J. L., 1999b. Tide response and wave distortion in Xiangshan Bay II: Numerical modeling study in the Xiangshan Bay. *Acta Oceanogica Sinica*, **21**: 2 (in Chinese with English abstract).

Dong, L. X., and Su, J. L., 2000. Salinity distribution and mixing in Xiangshan Bay I: Salinity distribution and circulation pattern. *Oceanologia et Limnologia Sinica*, **31**: 157-158 (in Chinese with English abstract).

Friedrichs, C. T., and Aubrey, D. G., 1988. Non-linear tidal distortion in shallow well-mixed estuaries: A synthesis. *Estuarine, Coastal and Shelf Science*, **27** (5): 521-545, DOI: 10.1016/0272-7714(88)90082-0.

Friedrichs, C. T., and Aubrey, D. G., 1994. Tidal propagation in strongly convergent channels. *Journal of Geophysical Research*, **99**: 3321-3336, DOI: 10.1029/93JC03219.

Friedrichs, C. T., and Madsen, O. S., 1992. Nonlinear diffusion of the tidal signal in frictionally dominated embayments. *Journal of Geophysical Research*, **97**: 5637-5650, DOI: 10.1029/92JC00354.

Gao, S., Xie, Q., and Feng, Y., 1990. Fine-grained sediment transport and sorting by tidal exchange in Xiangshan Bay, Zhejiang, China. *Estuarine, Coastal and Shelf Science*, **31**: 397-409, DOI: 10.1016/0272-7714(90)90034-O.

Huang, H. S., Chen, C. S., Blanton, J. O., and Andrade, F. A., 2008. A numerical study of tidal asymmetry in Okatee Creek, South Carolina. *Estuarine, Coastal and Shelf Science*, **78**: 190-202, DOI: 10.1016/j.ecss.2007.11.027.

Lanzoni, S., and Seminara, G., 1998. On tide propagation in convergent estuaries. *Journal of Geophysical Research*, **103**: 30793-30812, DOI: 10.1029/1998JC900015.

LeBlond, P. H., 1978. On tidal propagation in shallow rivers. *Journal of Geophysical Research*, **83**: 4717-4721, DOI: 10.1029/JC083iC09p04717.

Nicolle, A., and Karpytchev, M., 2007. Evidence for spatially variable friction from tidal amplification and asymmetry in the Pertuis Breton (France). *Continental Shelf Research*, **27**: 2346-2356, DOI: 10.1016/j.csr.2007.06.005.

Nidzieko, N. J., 2010. Tidal asymmetry in estuaries with mixed semidiurnal/diurnal tides. *Journal of Geophysical Research*, **115**, C08006, DOI: 10.1029/2009JC005864.

Nidzieko, N. J., 2012. Tidal asymmetry and velocity skew over tidal flats and shallow channels within a macrotidal river delta. *Journal of Geophysical Research*, **117**, C03001, DOI: 10.1029/2011JC007384.

Parker, B. B., 1991. The relative importance of the various nonlinear mechanisms in a wide range of tidal interactions (review). In: *Tidal Hydrodynamics*. Parker, B. B., ed., Wiley, New York, 237-268.

Pietrzak, J., Jakobson, J. B., Burchard, H., Vested, H. J., and Petersen, O., 2002. A three-dimensional hydrostatic model for coastal and ocean modeling using a generalized topography following co-ordinate system. *Ocean Modelling*, **4**: 173-205, DOI: 10.1016/S1463-5003(01)00016-6.

Sheng, J., and Wang, L., 2004. Numerical study of tidal circulation and nonlinear dynamics in Lunenburg Bay, Nova Scotia. *Journal of Geophysical Research*, **109**, C10018, DOI: 10.1029/2004JC002404.

Shetye, S. R., and Gouviea, A. D., 1992. On the role of geometry of cross-section in generating flood-dominance in shallow estuaries. *Estuarine, Coastal and Shelf Science*, **35**: 113-126, DOI: 10.1016/S0272-7714(05)80107-6.

Song, D. H., Wang, X. H., Kiss, A. E., and Bao, X. W., 2011. The contribution to tidal asymmetry by different combinations of tidal constituents. *Journal of Geophysical Research*, **116**, C12007, DOI: 10.1029/2011JC007270.

Speer, P. E., and Aubrey, D. G., 1985. A study of non-linear tidal propagation in shallow inlet/estuarine systems Part II: Theory. *Estuarine, Coastal and Shelf Science*, **21**: 207-224, DOI: 10.1016/0272-7714(85)90097-6.

Spitz, Y. H., and Klinck, J. M., 1998. Estimate of bottom and surface stress during a spring-neap tide cycle by dynamical assimilation of tide gauge observations in the Chesapeake Bay. *Journal of Geophysical Research*, **103**: 12761-12782, DOI: 10.1029/98JC00797.

van Maraen, D. S., and Gerritsen, H., 2012. Residual flow and tidal asymmetry in the Singapore Strait, with implications for resuspension and residual transport of sediment. *Journal of Geophysical Research*, **117**, C04021, DOI: 10.1029/2011JC007615.

Wang, Z. B., Jeuken, M. C. J. L., Gerritsen, H., de Vriend, H. J., and Kornman, B. A., 2002. Morphology and asymmetry of the vertical tide in the Westerschelde Estuary. *Continental Shelf Research*, **22**: 2599-2609, DOI: 10.1016/S0278-4343(02)00134-6.

Xu, P., Liu, Z. Y., Mao, X. Y., and Jiang, W. S., 2012. Estimation of vertical eddy viscosity and bottom drag coefficients in tidally energetic narrow bay. *Periodical of Ocean University of China*, **43**: 1-7 (in Chinese with English abstract).

Zhang, L. X., Jiang, X. S, and Cai, Y. H., 2008. Characteristics of nutrient distributions and eutrophication in seawater of the Xiangshan Harbor. *Marine Environmental Science*, **27**: 488-491 (in Chinese with English abstract).

Zheng, L. Y., Chen, C. S., and Liu, H. D., 2003. A modeling study of the Satilla River Estuary, Georgia. I: Flooding-drying process and water exchange over the salt marsh-estuary-shelf complex. *Estuaries*, **26**: 651-669, DOI: 10.1007/BF02711977.

Zhu, J. Z., and Cao, Y., 2010. Application of FVCOM for computation of 3D tidal flow and salinity in Xiangshan Bay. *Marine Environmental Science*, **29**: 899-903 (In Chinese with English abstract).

(Edited by Xie Jun)